

# Range extension of a scanning confocal chromatic sensor for precise robotic inline 3D measurements

Daniel Wertjanz, Nikolaus Berlakovich, Ernst Csencsics and Georg Schitter, *Senior Member, IEEE*

*Christian Doppler Laboratory for Precision Engineering for Automated In-Line Metrology*

*Automation and Control Institute (ACIN), Technische Universität Wien*

Vienna, Austria

wertjanz@acin.tuwien.ac.at

**Abstract**—This paper introduces the intermediate range extension concept of a precision 3D measurement module for robotic inline measurements. A scanning confocal chromatic sensor (SCCS) is integrated with a magnetically levitated and actuated measurement platform (MP) for enabling the acquisition of 3D images with sub-micrometer resolution. The MP is capable of tracking a sample surface in the out-of-plane degrees of freedom to actively compensate for relative motion between the SCCS and the sample. Using the MP to position the SCCS at multiple measurement locations, 3D measurements of the surface structure under test are acquired with overlapping regions between neighbouring frames. A 3D image processing and parallel registration algorithm is implemented in order to ensure a robust and precise merging of the individual 3D images. Experimental results demonstrate an extension of the SCCS' lateral measurement range by a factor 3 to about  $500 \times 500 \mu\text{m}^2$  while achieving sub-micrometer resolution in the entire range-extended 3D measurement. Compared to state-of-the-art repositioning with the robot, the measurement accuracy is increased by a factor of 9.

**Index Terms**—Mechatronics, system integration, precision inline 3D measurements

## I. INTRODUCTION

The demand for precision, throughput and quality assurance in the industrial high-tech manufacturing sector is steadily increasing [1]. Flexible and precise inline measurements of industrially produced goods are crucial for enabling the demanded 100% quality control [2], [3], which allows realtime optimization of production parameter settings to enhance the overall throughput as well as the production yield [4], [5].

Precise 3D surface measurements are considered as a key technology, because properties, such as topography and roughness, frequently serve as quality indicators in the semiconductor, automotive and consumer electronics sector [6]–[9]. An approach to flexibly position a 3D measurement tool (MT) at arbitrary measurement spots on a freeform

This project is partially funded by the Hochschuljubilaeumsfonds of the city of Vienna, Austria under the project number H-260744/2020. The financial support by the Christian Doppler Research Association, the Austrian Federal Ministry for Digital and Economic Affairs, and the National Foundation for Research, Technology and Development, as well as MICRO-EPSILON MESSTECHNIK GmbH & Co. KG and ATENSOR Engineering and Technology Systems GmbH is gratefully acknowledged. The authors are with the Christian Doppler Laboratory for Precision Engineering for Automated In-Line Metrology, Automation and Control Institute (ACIN), Technische Universität Wien, 1040 Vienna.

surface [10] and to extend its measurement range [11] is by employing industrial robots. Current optical robotic 3D measurement systems achieve resolutions down to  $50 \mu\text{m}$  [12], [13]. However, robots themselves are not suitable for 3D surface measurements with single- or even sub-micrometer resolution [14] as the positioning accuracy of modern industrial robots is in the range of several tens of micrometers [15].

Moreover, environmental vibrations, such as present in an industrial production line, are considered as a major challenge. Relative motion between the MT and the sample surface can be caused by these disturbing vibrations, corrupting 3D measurements due to motion blur [16]. Therefore, precision 3D measurements are typically conducted in a vibration-free lab environment, making a 100% quality control of goods with structural sizes in the single-micrometer range usually impossible without impairing the production throughput.

Recently, a robotic inline measurement system for precise 3D surface inspection on freeforms in vibrational environments has been reported [17]. By means of active sample tracking, the integrated MAGLEV measurement platform (MP) compensates for disturbing vibrations and establishes lab-like conditions for the developed compact and lightweight scanning confocal chromatic sensor (SCCS) [18] mounted onto the MP.

With an operable robotic measurement system for high resolution 3D measurements available, the lateral measurement range of the SCCS ( $350 \times 250 \mu\text{m}^2$ ) represents a limitation for applications requiring larger lateral ranges. Using the robot for repositioning the MT and acquiring multiple partly overlapping 3D images [19] that are combined by image registration techniques [20], [21], may appear as a viable approach. However, the in relation to the positioning uncertainty of the robot comparably small lateral measurement range of the SCCS, may cause insufficient overlap regions between the individual 3D image and a decreased registration performance. For this reason, an intermediate and highly precise range extension concept is required.

The contribution of this paper is i) the integration of an intermediate range extension concept with the previously reported MP approach, ii) the registration of individual 3D images acquired at adjacent measurement locations, and iii) the experimental validation of the range-extended 3D mea-

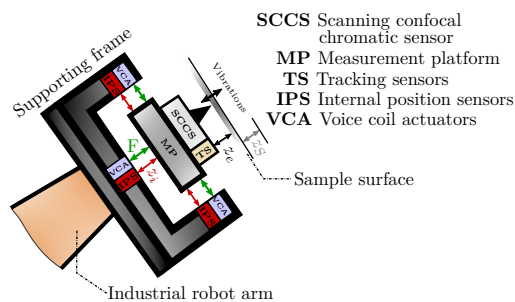
surement performance.

For a precise intermediate range extension the positioning range of the MP is tailored to move the MP over an enlarged lateral scan area, matched to the typical positioning uncertainty of an industrial robot.

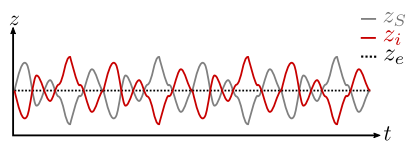
The remainder of this paper is structured as follows. Section II presents the integrated mechatronic design of the robotic inline precision 3D measurement system for operation in arbitrary robot poses. In Section III, the concept for extending the lateral range of the SCCS as 3D MT is described in detail. Experimental results of the robotic precision 3D measurement system are analyzed and discussed in Section IV. Finally, Section V concludes the paper.

## II. MEASUREMENT MODULE FOR ROBOTIC APPLICATIONS

The system concept of precise robot-based inline 3D measurements on freeform surfaces within vibration-prone environments is illustrated in Fig.1. Acting as a robot end-effector, the measurement module comprises a precision 3D MT mounted on a MAGLEV MP with tracking sensors measuring the relative position of the 3D MT to the sample surface. Independent on the actual robot pose, a constant alignment of the MT relative to the sample surface under test is maintained by means of feedback control. The resulting contactless stiff link between MT and sample surface actively compensates for relative motion and establishes lab-like conditions for the 3D MT directly in vibrational environments such as an industrial production line.



(a) Measurement module for robotic applications.



(b) According position signals.

Fig. 1: System concept of robotic inline precision 3D measurements on freeform surfaces. a) By maintaining a constant alignment  $z_e$  between the MT and the sample surface, disturbing vibrations  $z_S$  are actively compensated. b) In the internal position signal  $z_i$ , the tracking motion is visible, compensating the sample vibrations  $z_S$ .

Considering the concept in Fig. 1, Fig. 2 shows the implemented measurement system prototype with an active sample-tracking MP [17]. An industrial robot arm (KR 10 R900-2, KUKA AG, Augsburg, Germany) is used to coarsely align the measurement system to an arbitrary spot on a sample surface. To ensure a robust 3D image registration when moving the robot arm, the SCCS' lateral scan area is desired to be a factor of 10 higher than the positioning uncertainty of the robot arm. Assuming a typical robot position uncertainty of  $50 \mu\text{m}$  [15], a lateral scan area of  $500 \times 500 \mu\text{m}^2$  is targeted.

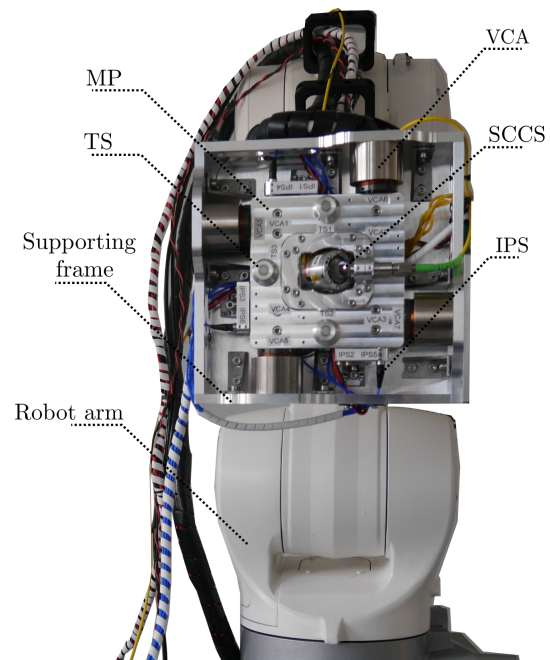


Fig. 2: Robotic inline measurement system for precise 3D surface inspection in vibrational environments. The vibration-compensating measurement module, with the SCCS as 3D MT on the MP, is mounted on an industrial robot arm.

### A. Scanning confocal chromatic sensor

In order to achieve the targeted precision 3D measurements, the lightweight SCCS in Fig. 3 has been developed as a 3D MT [18]. Having a compact size of  $75 \times 63 \times 55 \text{ mm}^3$ , the SCCS is tailored for integration onto the MAGLEV MP. By manipulating the optical path of a high precision 1D confocal chromatic sensor (CCS) with a high performance fast steering mirror (FSM) [22], the measuring light spot is scanned across the sample surface to be inspected. A multi-input-multi-output (MIMO)  $H_\infty$  controller is implemented to achieve high performance motion control of the two FSM axes. An efficient and dense scanning motion is achieved by applying Lissajous trajectories to the FSM axes. Using a data-driven image reconstruction procedure, the FSM deflection

angles and the correspondingly measured distances are combined to obtain an accurate 3D surface measurement. The measurement volume of about  $350 \times 250 \times 1800 \mu\text{m}^3$  can be imaged with frame rates of up to 1 fps. High resolution scans with a lateral and axial resolution of down to  $2.5 \mu\text{m}$  and  $76 \text{ nm}$ , respectively, can be performed. A detailed discussion on the SCCS' system design, as well as an experimental validation of the achieved performance, can be found in [18].

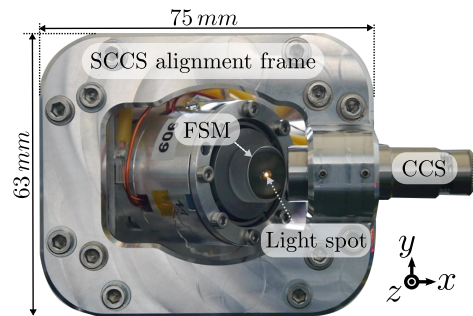


Fig. 3: Compact SCCS for precision 3D measurements. Using a high performance FSM, the light spot of the CCS is precisely scanned across the sample surface for acquiring the topography.

### B. Module for active sample-tracking

Being a core component of the entire measurement system, the integrated tracking module comprises a MAGLEV MP. Eight identical voice coil actuators (VCAs) are placed around the MP, yielding a balanced system design and enabling operation in arbitrary orientations [23]. The MP is freely floating and actuated within the air gaps of the VCAs. The tracking module comprises six capacitive internal position sensors (IPSs), measuring the MP's position relative to the supporting frame. This measured internal position is used in feedback control to maintain a free-floating position with respect to the supporting frame (stabilization mode) when repositioning the robot. Additionally, three capacitive tracking sensor (TS) are included, measuring the MP's out-of-plane position relative to a sample surface. Thus, the system is capable of actively tracking a sample surface in the out-of-plane degrees of freedom (DoFs), while it is stabilized in-plane. As a high tracking performance of the MP is desired, 600 Hz proportional-integral-derivative (PID) position controllers are designed and implemented to individually control each DoF. The MP can be positioned with a resolution of about  $17 \text{ nm rms}$ , either to its supporting frame or a sample surface.

Considering the lateral range of a single 3D measurement ( $350 \times 250 \mu\text{m}^2$ ) acquired by the SCCS, a MP repositioning of about  $\pm 125 \mu\text{m}$  in the DoFs  $x$  and  $y$  is sufficient to achieve the targeted area of  $500 \times 500 \mu\text{m}^2$  with overlapping 3D images. Therefore, the lateral actuation range of the MP is limited

to  $\pm 125 \mu\text{m}$ , maintaining a margin in the actuation range and avoiding mechanical damage.

### III. INTERMEDIATE MEASUREMENT RANGE EXTENSION

As previously discussed in Section I, a MP-based intermediate range extension of the SCCS' lateral scan area is necessary to ensure sufficiently large overlap regions between neighbouring 3D image frames when repositioning the robot. Figure 4 illustrates the flow chart of the proposed intermediate range extension concept, with the 3D image acquisition at multiple measurement location achieved by repositioning the MP and the subsequent image processing as the two main tasks described in the following.

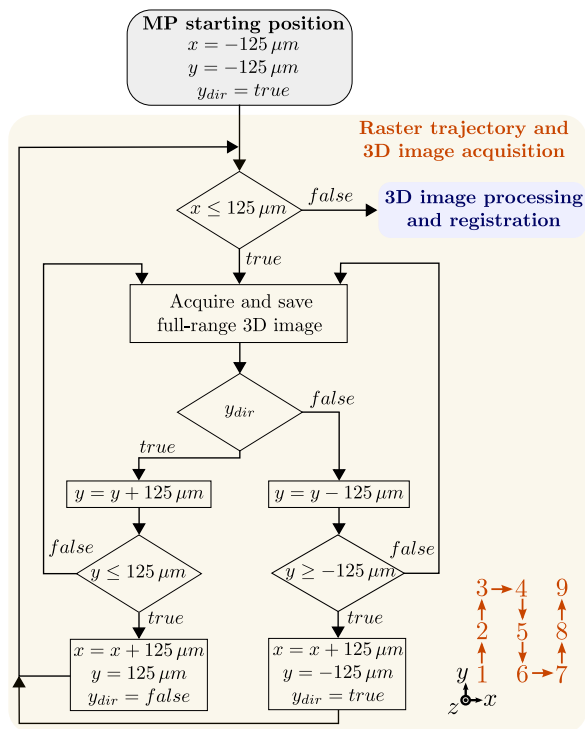
#### A. Acquisition of overlapping 3D images

By using the MP to position the SCCS at multiple measurement spots, fast and precise repositioning is enabled, yielding an efficient intermediate range extension. As indicated by the process on the left in Fig. 4a, a  $125 \mu\text{m}$ -raster pattern with  $3 \times 3$  measurement locations is applied to the MP. In order to achieve a smooth and efficient repositioning of the MP, minimum jerk trajectories are applied to the MP's in-plane position control. At each measurement location, indicated by the numbers 1 to 9 on the bottom-right in Fig. 4a, a full-range 3D image is acquired, resulting in nine individual 3D images with a defined overlap region between the neighbouring frames. During a 3D measurement performed with the SCCS, a constant alignment of the SCCS relative to the sample surface is desired. Therefore, the MP operates in tracking mode, i.e it actively tracks the sample surface in the three out-of-plane DoFs  $z$ ,  $\phi_x$  and  $\phi_y$ .

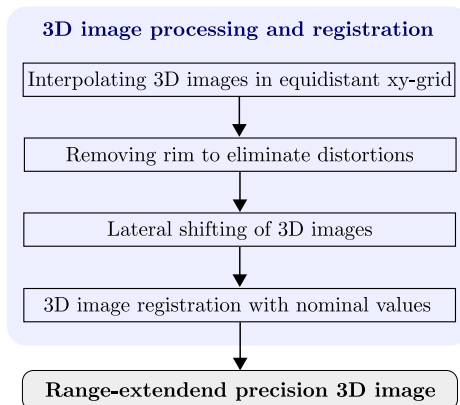
#### B. 3D image processing and registration

Subsequently to the image acquisition, the 3D image processing and registration procedure in Fig. 4b. Firstly, the individual 3D image frames are interpolated into an equidistant  $xy$ -grid with a reduced number of data points ( $350 \times 250$ ), reducing the measurement noise as well as the computation effort for the following registration algorithm. Next, slight distortions at the 3D image border are eliminated by removing a rim with a width of  $30 \mu\text{m}$ , maintaining overlap regions of about 20% of the full-range 3D image. To provide the registration algorithm the required nominal position of the individually performed 3D measurements, each image frame is shifted by the MP's  $xy$ -position in which it has been measured.

As in-plane TSs are not yet integrated on the MP, the relative motion of a sample surface in the DoFs  $x$ ,  $y$  and  $\phi_z$  can not be monitored. Thus, position uncertainties may occur when merging the individual 3D images using their nominal positions. In order to reduce the resulting overlap mismatch between the 3D images, a parallel registration algorithm is used for the precise registration of each 3D image [21]. In its original version, the algorithm additionally propagates the images along their surface normals, which is not necessary in this application due to actively tracking the sample in the three



(a) MP-based repositioning of the SCCS and 3D image acquisition.



(b) 3D image processing and registration.

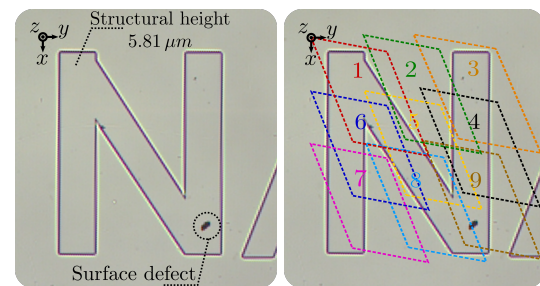
Fig. 4: Flow chart of the intermediate measurement range extension process. a) The MP is laterally moved ( $x$ - and  $y$ -axis) in a raster pattern across the sample surface and 3D images are acquired. b) A 3D image processing and registration routine is used to efficiently and robustly merge the individual 3D image frames.

out-of-plane DoFs and therefore omitted. The registration is carried out in an iterative manner and takes about 300 ms on a personal computer.

#### IV. EXPERIMENTAL EVALUATION OF THE RANGE-EXTENDED 3D IMAGING PERFORMANCE

The proposed concept for extending the 3D imaging range of the SCCS from Section III is experimentally validated by comparing its performance with a robot-based state-of-the-art range extension approach. Therefore, a silicon step height standard (Nanuler Calibration Standard, Applied NanoStructures Inc., Mountain view, CA, USA) with a nominal structural height of  $5.81 \mu\text{m}$  is used. In Fig. 5a, a microscope image of the first letter of the manufacturer's logo is shown, which is chosen as test structure. As can be clearly seen, a surface defect is located on the bottom-right.

Considering the concept discussed in Section III, Fig. 5b shows the acquisition of the  $3 \times 3$  individual and overlapping 3D image frames. The raster motion and the resulting nine SCCS' measurement locations are indicated by the numbered frames. Note that the rhomboidal shape of the SCCS' lateral measurement area is caused by geometrical constraints together with mounting tolerances [18]. Each individual 3D measurement is performed by applying driving frequencies of 5.7 Hz and 4.3 Hz to the tip and tilt axis of the FSM, yielding a dense Lissajous scan pattern, high lateral resolution and an efficient measurement time of  $T = 10 \text{ s}$  [17], [18].



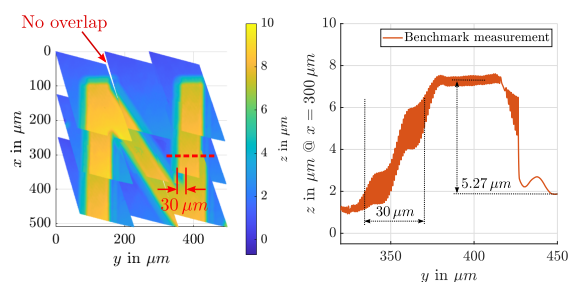
(a) Microscope image of the test structure. (b) SCCS' measurement locations.

Fig. 5: Microscope image of the test structure and the SCCS' measurement locations. a) shows the first letter of the manufacturer's logo with a structural height of  $5.81 \mu\text{m}$  and a surface defect on the letter "N". In b), the raster motion and the resulting SCCS' measurement locations are indicated by the numbered frames.

##### A. Robot-based benchmark measurement

In a first step, a robot-based range-extended 3D measurement is performed, which serves as a benchmark for the proposed intermediate range extension concept from Section III. Therefore, the raster pattern routine of Fig. 4a is not applied to the MP but to the robot position controller. Using the nominal values of the individually performed 3D measurements, each image frame is shifted by the robot's  $xy$ -position in which it has been measured. The resulting robot-based range-extended 3D measurement is illustrated in Fig. 6a. Due to the limited position accuracy of the industrial robot, a small non-overlap

region occurs in the top-left section. Moreover, a lateral overlap mismatch of about  $30\mu\text{m}$  is visible at the bottom-right. The dashed red line indicates the cross section analyzed in Fig. 6b. As can be seen, an incorrect sample height of  $5.27\mu\text{m}$  with respect to the ground plane on the right side of the structure is measured, yielding a height measurement error of  $540\text{nm}$ . The height interpolation in the region in which the aforementioned lateral overlap mismatch of about  $30\mu\text{m}$  occurs, causes the visible noise in the height signal  $z$ . Hence, the relatively high position uncertainty of the industrial robot in comparison to the SCCS lateral measuring range, makes this robot-based approach inappropriate for the targeted enlarged 3D measurements, especially for surface structures with lateral dimensions on the single-micrometer scale.



(a) Robot-based repositioning. (b) Cross section at  $x = 300\mu\text{m}$ .

Fig. 6: Benchmark measurement. a) Results for a robot-based repositioning of the SCCS. Lateral shifting of the acquired 3D images by the nominal values of the robot arm results in a non-overlap region between two individual 3D image frames. b) shows the cross section at  $x = 300\mu\text{m}$  in the interval  $y \in [330\mu\text{m}, 450\mu\text{m}]$ , indicated by the dashed red line in a). An incorrect sample height of  $5.27\mu\text{m}$  is measured. The lateral overlap mismatch of  $30\mu\text{m}$  cause measurement noise in the height signal  $z$ .

### B. Intermediate range extension concept

Following the proposed intermediate range extension concept, the raster pattern routine (see Fig. 4a) is applied to the MP and at each measurement location in Fig. 5b a 3D image is acquired. The acquisition time of the  $3 \times 3$  individual 3D images is about  $9T = 90\text{s}$  as the time for the fast MP repositioning ( $50\text{ms}$ ) is neglectable. Subsequently, the 3D image processing algorithm is performed.

In Fig. 7a, the result for merging the individual 3D images solely by their nominal positions, i.e. before 3D image registration, is shown. Note that the top-left corner of the merged 3D image is set to  $(x = 0\mu\text{m}/y = 0\mu\text{m})$  for reasons of consistency (see coordinate system in Fig. 5). An overlap mismatch between the 3D image frames is caused by positioning uncertainties of the MP relative to the sample surface (see Section III). The red dashed cross section at  $x = 155\mu\text{m}$  is analyzed in Fig. 7c (red), with the noise in the

interval of  $y \in [260\mu\text{m}, 300\mu\text{m}]$  clearly indicating an overlap mismatch due to position uncertainties. Moreover, the defined structural height of  $5.81\mu\text{m}$  is not measured correctly. The measurement error in the interval of  $y \in [360\mu\text{m}, 380\mu\text{m}]$  is most probably caused by light diffraction and shading effects at the silicon edges.

Applying the 3D image registration algorithm [21] to the nominally positioned 3D images in Fig. 7a, the corrected 3D measurement of the test structure is shown in Fig. 7b. The entire registration process is performed in only  $300\text{ms}$  on a personal computer. An extended SCCS' lateral measurement area of about  $500 \times 500\mu\text{m}^2$  is achieved, which meets the targeted specifications defined in Section II. Again, the red dashed cross section at  $x = 155\mu\text{m}$  is analyzed in Fig. 7c (black). As it can be clearly seen, the noise in the interval of  $y \in [260\mu\text{m}, 300\mu\text{m}]$  is considerably reduced, indicating a small overlap mismatch. In the intermediate range-extended 3D image, a structural height of  $5.87\mu\text{m}$  is measured, corresponding to a measurement error of only  $60\text{nm}$ . Compared with the height error in the benchmark measurement in Fig. 6b, the measurement accuracy is improved by a factor of 9. In addition, the small defect (see Fig. 5a) on the test structure's surface is clearly visible, highlighting the system's ability to perform robot-based precision 3D measurements for surface quality assurance.

In summary, the experimental results demonstrate that the proposed concept successfully extends the SCCS' lateral measurement area by a factor of 3 to  $500 \times 500\mu\text{m}^2$  without impairing its sub-micrometer measurement.

## V. CONCLUSION

In this paper, an intermediate range extension concept of a SCCS for precise robotic inline 3D measurements is presented. The 3D MT is mounted to a MAGLEV MP, which is capable of actively tracking a sample surface in the out-of-plane DoFs. As the SCCS' lateral scan area is relatively small compared to the position uncertainty of an industrial robot, a robot-based measurement range extension may cause insufficient overlap regions between the individual 3D measurements. Therefore, the MP is used to precisely position the 3D MT at multiple measurement locations, enabling an efficient pre-extension of the SCCS' lateral scan area as an intermediate step. Precision 3D images are acquired at defined measurement spots with a total acquisition time of about  $90\text{s}$ , resulting in individual 3D measurements with overlap regions of at least  $20\%$  between neighbouring image frames. An efficient and robust parallel registration algorithm is implemented, reducing the uncertainty of the  $3 \times 3$  nominally positioned individual 3D images. Experimental results demonstrate an extension of the SCCS' scan area by a factor of 3 to  $500 \times 500\mu\text{m}^2$ , while achieving a measurement error of only  $60\text{nm}$  in the entire range-extended 3D measurement and demonstrating the ability to successfully measure surface defects. Compared to a solely robot-based range extension, the proposed concept boosts the measurement accuracy by a factor of 9.

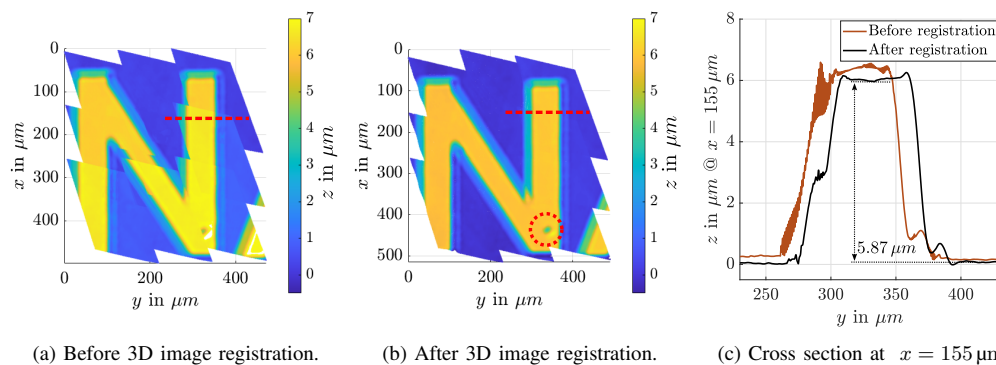


Fig. 7: Experimental results of the intermediate range extension concept. a) shows the nominally positioned 3D image frames without registration. A mismatch in the overlapping regions can be seen, whereas the surface defect on the bottom-right is hardly observable. In b), the result after 3D data registration [21] is illustrated. The defect on the surface structure (red dashed ring) is clearly visible. c) shows the cross section at  $x = 155 \mu\text{m}$  in both range-extended 3D measurements. After the 3D data registration, the position noise due to overlap mismatches is significantly reduced.

Future work includes the repositioning of the entire measurement module with the robot arm and the registration of multiple range-extended 3D measurements. In this way, the flexibility to precisely inspect surface structures with large lateral dimensions will be enabled.

#### REFERENCES

- [1] T. Uhrmann, T. Matthias, M. Wimplinger, J. Burggraf, D. Burgstaller, H. Wiesbauer, and P. Lindner, "Recent progress in thin wafer processing," in *2013 IEEE International 3D Systems Integration Conference (3DIC)*, 2013, pp. 1–8.
- [2] D. Imkamp, R. Schmitt, and J. Berthold, "Blick in die Zukunft der Fertigungsmesstechnik - Die VDI/VDE-GMA Roadmap Fertigungsmesstechnik 2020," *Technisches Messen*, vol. 10, no. 79, 2012.
- [3] R. Schmitt and F. Moenning, "Ensure success with inline-metrology," in *XVIII IMEKO World Congress - Metrology for a Sustainable Development*, 2006.
- [4] W. Gao, H. Haitjema, F. Fang, R. Leach, C. Cheung, E. Savio, and J. Linares, "On-machine and in-process surface metrology for precision manufacturing," *CIRP Annals*, vol. 68, no. 2, pp. 843–866, 2019.
- [5] M. Grasso and B. Colosimo, "Process defects and in situ monitoring methods in metal powder bed fusion: a review," *Measurement Science and Technology*, vol. 28, p. 044005, 2017.
- [6] A. Yogeswaran and P. Payeur, "3d surface analysis for automated detection of deformations on automotive body panels," in *New Advances in Vehicular Technology and Automotive Engineering*. IntechOpen, 2012.
- [7] T.-F. Yao, A. Duenner, and M. Cullinan, "In-line dimensional metrology in nanomanufacturing systems enabled by a passive semiconductor wafer alignment mechanism," *Journal of Micro- and Nano-Manufacturing*, vol. 5, no. 1, 2016.
- [8] G. Sansoni, M. Trebeschi, and F. Docchio, "State-of-the-art and applications of 3d imaging sensors in industry, cultural heritage, medicine, and criminal investigation," *Sensors (Basel, Switzerland)*, vol. 9, pp. 568–601, 2009.
- [9] H. Schwenke, U. Neuschaefer-Rube, T. Pfeifer, and H. Kunzmann, "Optical methods for dimensional metrology in production engineering," *CIRP Annals*, vol. 51, no. 2, pp. 685–699, 2002.
- [10] E. Savio, L. D. Chiffre, and R. Schmitt, "Metrology of freeform shaped parts," *CIRP Annals*, vol. 56, no. 2, pp. 810–835, 2007.
- [11] J. Rejc, J. Cinkelj, and M. Muni, "Dimensional measurements of a gray-iron object using a robot and a laser displacement sensor," *Robotics and Computer-Integrated Manufacturing*, vol. 25, no. 2, pp. 155–167, 2009.
- [12] S. Yin, Y. Ren, Y. Guo, J. Zhu, S. Yang, and S. Ye, "Development and calibration of an integrated 3d scanning system for high-accuracy large-scale metrology," *Measurement*, vol. 54, pp. 65–76, 2014.
- [13] G. B. de Sousa, A. Olabi, J. Palos, and O. Gibaru, "3d metrology using a collaborative robot with a laser triangulation sensor," *Procedia Manufacturing*, vol. 11, pp. 132–140, 2017.
- [14] E. Csencsics, M. Thier, S. Ito, and G. Schitter, "Supplemental peak filters for advanced disturbance rejection on a high precision endeffector for robot-based inline metrology," *IEEE/ASME Transactions on Mechatronics (Early Access)*, 2021.
- [15] U. Schneider, M. Drust, M. Ansaloni, C. Lehmann, M. Pellicciari, F. Leali, J. Gunnink, and A. Verl, "Improving robotic machining accuracy through experimental error investigation and modular compensation," *The International Journal of Advanced Manufacturing Technology*, vol. 85, pp. 1–13, 2014.
- [16] R. Saathof, M. Thier, R. Hainisch, and G. Schitter, "Integrated system and control design of a one dof nano-metrology platform," *Mechatronics*, vol. 47, pp. 88–96, 2017.
- [17] D. Wertjanz, E. Csencsics, and G. Schitter, "Three-dof vibration compensation platform for robot-based precision inline measurements on free-form surfaces," *IEEE Transactions on Industrial Electronics*, vol. 69, no. 1, pp. 613–621, 2022.
- [18] D. Wertjanz, T. Kern, E. Csencsics, G. Stadler, and G. Schitter, "Compact scanning confocal chromatic sensor enabling precision 3-d measurements," *Appl. Opt.*, vol. 60, no. 25, pp. 7511–7517, 2021.
- [19] A. Paoli and A. V. Rationale, "Large yacht hull measurement by integrating optical scanning with mechanical tracking-based methodologies," *Robotics and Computer-Integrated Manufacturing*, vol. 28, no. 5, pp. 592–601, 2012.
- [20] P. J. Besl and N. D. McKay, "Method for registration of 3-d shapes," in *Sensor fusion IV: control paradigms and data structures*, vol. 1611. International Society for Optics and Photonics, 1992, pp. 586–606.
- [21] N. Berlakovich, E. Csencsics, M. Fuerst, and G. Schitter, "Iterative parallel registration of strongly misaligned wavefront segments," *Opt. Express*, vol. 29, no. 21, pp. 33 281–33 296, 2021.
- [22] E. Csencsics, J. Schlarp, T. Schopf, and G. Schitter, "Compact high performance hybrid reluctance actuated fast steering mirror system," *Mechatronics*, vol. 62, p. 102251, 2019.
- [23] D. Wertjanz, E. Csencsics, J. Schlarp, and G. Schitter, "Design and control of a maglev platform for positioning in arbitrary orientations," in *2020 IEEE/ASME International Conference on Advanced Intelligent Mechatronics (AIM)*, 2020, pp. 1935–1942.